Incorporation of Hydrophobic Dyes within Cellulose Acetate and Acetate Phthalate Based Nanoparticles

Peter Schulze, Martin Gericke,* Friedrich Scholz, Holger Wondraczek, Peter Miethe, Thomas Heinze*

Polysaccharide based nanoparticles (NP) have demonstrated a unique potential for biomedical and biotechnological applications. Various functionalities can be covalently linked to these NP, however, physical entrapment of functional compounds is still a highly desired approach, e.g., for drug delivery. Using different dyes, it is demonstrated how hydrophobic compounds can be incorporated into composite particles derived from cellulosic esters and how the particle properties are affected by the composition. The dye loaded NP are studied by UV–vis spectroscopy to gain insight in the interaction of the hydrophobic compounds with the cellulosic matrix. By using functional cellulose derivatives, in particular carboxylate group bearing acetate phthalates, it is possible to introduce reactive moieties on the NP surface that can be exploited for coupling additional functionalities such as antibodies. By this approach, NP can be obtained that are well suited as dye labels in immunoassay applications.

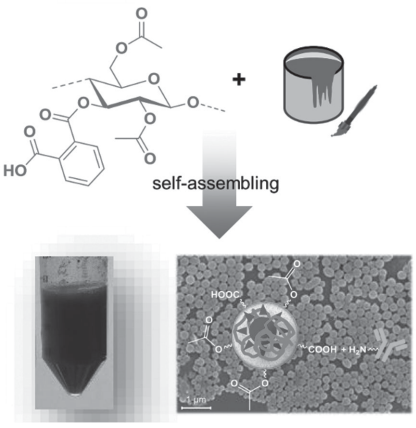

1. Introduction

Hydrophobic polysaccharide derivatives, such as esters of monocarboxcylic acids, alkyl- and phenyl carbonates, and acetals derived from cellulose, dextran, and xylan, are capable of forming well-defined spherical nanoparticles (NP) with diameters in the range of ≈50–1000 nm by self-assembling.[1–4] The self-assembling may be achieved by different techniques. Dialysis of the polysaccharide derivatives dissolved in a dipolar aprotic solvent against water induces regeneration of the hydrophobic polymers by a slow exchange of solvent against nonsolvent.[5] A similar effect is achieved by slowly dropping a solution of the hydrophobic polysaccharide derivatives into water or vice versa.[1,3,6] Moreover, NP with a very narrow size distribution can be obtained using an ultrasound assisted emulsion-evaporation process.[7,8]

NP based on hydrophobic polysaccharide derivatives are of great interest for medical, pharmaceutical, and biotechnological applications. They are easy to prepare and taken up by cells without showing cytotoxicity.[9] In order to introduce specific functionalities (e.g., sensoring, drug delivery, antigen detection, and stimuli responsiveness), different active molecules (e.g., dyes, drugs, antibodies, and ionic substituents) have been attached covalently either directly to the particles or to the hydrophobic

P. Schulze, Dr. M. Gericke, Dr. H. Wondraczek, Prof. T. Heinze
Institute of Organic Chemistry and Macromolecular Chemistry
Friedrich Schiller University of Jena
Centre of Excellence for Polysaccharide Research
Humboldtstraße 10, D-07743 Jena, Germany
E-mail: martin.gericke@uni-jena.de;
thomas.heinze@uni-jena.de
P. Schulze, Dr. P. Miethe
fzmb GmbH
Forschungszentrum für Medizintechnik und Biotechnologie
Geranienweg 7, D-99947 Bad Langensalza, Germany
Dr. F. Scholz
Senova Gesellschaft für Biowissenschaft und Technik mbH
Industriestraße 8, D-99427 Weimar, Germany

Macromol. Chem. Phys. **2016**, DOI: 10.1002/macp.201600160

polysaccharide derivatives prior to the self-assembling process.[10–13]

Physical entrapment is a highly desired and facile alternative for loading polysaccharide based NP with a broad variety of active substances. It would enable higher loading capacities compared to covalent immobilization. Moreover, the release of compounds from such composite NP, which is desired for drug delivery, would not require chemical cleavage; it can be achieved by simple disintegration and/or dissolution of the NP. Using pyrene as a fluorescent probe, it has been demonstrated that the interior of NP, prepared by self-assembling of hydrophobic polysaccharide esters, is significantly less polar than the surrounding aqueous medium.[5] Thus, it is hypothesized that high amounts of hydrophobic compounds up to a ratio of 50 wt% may be incorporated simply by adding them to the polysaccharide ester solution during the self-assembling procedure.

This work focuses on the entrapment of hydrophobic dyes within NP derived from two different hydrophobic cellulose esters, namely cellulose acetate (CA) and cellulose acetate phthalate (CAPh). The latter features reactive carboxyl groups that can be employed for coupling of active molecules such as antibodies. The NP obtained were characterized by UV–vis spectroscopy to gain insight into the interaction between the polysaccharide ester matrix and incorporated hydrophobic compounds. The colored polysaccharide based NP are of great interest as nanolabels for lateral flow immunoassays.[12,14] Their suitability for the detection of C-reactive protein (CRP) in a lateral flow test system was evaluated in this work. Cellulose esters such as CA and CAPh are of great pharmaceutical importance as matrices for the stabilization and controlled release of hydrophobic drug molecules.[15] Thus, the study may also provide valuable information that can be exploited for preparing drug loaded polysaccharide based NP for drug delivery purposes.

2. Experimental Section

2.1. Materials

N,N-Dimethylacetamide (DMA) of anhydrous grade was purchased and from Acros Organics in sealed vessels containing molecular sieves. For UV–vis experiments, DMA and acetone were of spectrophotometric grade and purchased from Sigma-Aldrich. Cellulose 2.5 acetate (CA; $DS_{acetate}$ = 2.3, determined by perpropionylation and ^{1}H NMR spectroscopy as described in the literature.[16]; M_n = 59500 g mol^{-1} and M_w = 137900 g mol^{-1}, determined by size exclusion chromatography(SEC)) was obtained from Eastman Chemical Company. CAPh ($DS_{acetate}$ = 1.8 and $DS_{phthalate}$ = 0.7, determined by quantitative ^{13}C NMR spectroscopy; M_n = 29900 g mol^{-1} and M_w = 63600 g mol^{-1}, determined by SEC) was obtained (in its protonated form) from Sigma-Aldrich. The molecular weights of both cellulose esters (CA: M_n = g mol^{-1}, M_w = g mol^{-1}; CA: M_n = g mol^{-1}, M_w = g mol^{-1}) were determined by SEC.

2-Aminoanthraquinone (AA), sudan IV (SIV; solvent red, 24 C.I. 26105) and sudan black B (SB; solvent black 3, C.I. 26150) were purchased from Alfa Aesar. Deionized water was employed for all experiments related to the particle preparation. For analytical measurements such as particle size determination and UV-vis experiments, HPLC grade water (supplied by Carl Roth GmbH) was employed. For immunoassay related experiments, water (reverse osmosis quality) was obtained from a Millipore unit.

All buffer solutions were prepared with reverse osmosis grade water. Phosphate buffered saline (PBS; 1.2 mol L^{-1} NaCl, 0.3 mol L^{-1} phosphate, pH 7.3), phosphate buffered solution (PB; 0.3 mol L^{-1} or 0.03 mol L^{-1} phosphate, pH 6.5, 7.3, and 8.0), 2-(*N*-morpholino) ethanesulfonic acid buffered solution (MES; 0.3 mol L^{-1}, pH 5.5), and bicarbonate buffered solution (CBB; 0.3 mol L^{-1} carbonate, pH 9.5) were prepared from the corresponding salts obtained from Roth (Karlsruhe, Germany). The monoclonal antibodies antihuman CRP 6404 (anti-h CRP 6404) and antihuman CRP 6405 (anti-h CRP 6405, both monoclonal, IgG) were received from Medix (Espo, Finland). The human CRP antigen was obtained from BioTrend (Cologne, Germany). Casein buffer concentrate (CBC) was obtained from SDT (Baseweiler, Germany). Bovine serum albumin (BSA) was received from Serva (Heidelberg, Germany). Sulfo-*N*-hydroxysuccinimide (sulfo-NHS) was obtained from G Bioscience (St. Louis, USA). 1-Ethyl-3-(3-dimethylaminopropyl) carbodiimide hydrochloride (EDC) was purchased from PanReac AppliChem.

Sartorius AG (Göttingen, Germany) supplied the nitrocellulose membrane (CN 140). Backing card (60 mm), absorbent pad (cotton fiber membrane, 1.8 cm, grade 222), conjugate pad (glass fiber membrane, 1.2 cm, grade 8964), and sample pad (glass fiber membrane, 1.8 cm, grade 9864) were obtained from Ahlstrom (Helsinki, Finland).

2.2. Measurements

All measurements were performed in-house according to standardized procedures. The hydrodynamic diameter, polydispersity, and ζ-potential of the NP were measured by dynamic light scattering using a Zetasizer Nano ZS (Malvern Instruments) with an operating wavelength of 633 nm and detection angle of 173°. The values displayed represented the average of triplicate measurements. The mean particle size was approximated as the effective (Z-average) diameter and the width of the distribution as the polydispersity index (PDI) obtained by the cumulants method assuming spherical shape. The samples obtained by dialysis were diluted with HPLC grade water (1:9) before measurement. Each determination was performed in triplicate. For scanning electron microscopy (SEM) images, 10 µL of the NP suspension were placed on a mica surface, dried, and sputtered with platinum. The SEM images were recorded using a LEO 1450 VP (Zeiss). Cryogenic transmission electron microscopy (cryo-TEM) measurements were performed on an FEI Tecnai G2 20 cryo-TEM. Acceleration voltages were set to 120 kV. Samples were prepared on Quantifoil grids (3.5/1) after cleaning by argon plasma treatment for 120 s. A volume of 9.5 µL of the solutions was blotted by using a Vitrobot Mark IV. Samples were plunge-frozen in liquid

Macromol. Chem. Phys. **2016**, DOI: 10.1002/macp.201600160

ethane and stored under nitrogen before being transferred to the microscope utilizing a Gatan transfer stage. SEC was performed on an JASCO system (isocratic pump JASCO PU-980, JASCO RI-930 refractive index detector) with a PSS NOVEMA 300 column and a PSS NOVEMA 3000 column in series using DMSO with 0.5% LiBr as eluent (65 °C, flow rate: 0.5 mL min^{-1}) and pullulan as calibration standard.

2.3. Particle Preparation

The preparation of NP was carried out by a dialysis procedure according to the literature.[7] As a typical example (**CA-2_AA-1**), 20 mg CA and 10 mg AA were dissolved in 10 mL DMA. Dust particles were removed by centrifugation (8000 min^{-1}, 5 min) and the clear solution was dialyzed in a regenerated cellulose dialysis membrane (MWCO: 3500 g mol^{-1}, nominal flat width: 18 mm, Spectra/Por 3) against 1 L deionized water. Over a course of 15 h, the water was exchanged five times after equal intervals.

2.4. UV–Vis Spectroscopic Characterization

2.4.1. Aqueous Dye Solutions

Solutions of SB in DMA/water (HPLC grade) mixtures (10:0 to 1:9) with a dye concentration of 1×10^{-5} mol L^{-1} and 2×10^{-5} mol L^{-1} were prepared by dilution of SB stock solutions ($7.86 \cdot 10^{-4}$ mol L^{-1}) in DMA. As an example, 127 µL of stock solution were placed in a 10 mL volumetric flask together with 8.873 µL DMA and 1 mL water. The residual volume, resulting from volume contractions, was filled with a DMA/water mixture of the desired mixing ratio (9:1) to yield a solution of 1×10^{-5} mol L^{-1} SB in DMA/water (9:1). The solutions obtained were measured using a PerkinElmer Lambda 25 UV–vis and quartz glass cuvettes. Extinction coefficients were derived by measuring the absorbance at two dye concentrations.

2.4.2. Cellulose Acetate Phthalate Films

Opaque CAPh/SB films were prepared by regeneration from DMA by solvent exchange with water. CAPh (0.5 mol L^{-1}) and different amounts of SB (0.04, 0.02, 0.01, and 0.005 mol L^{-1}) were dissolved in 1 mL DMA. Using a doctor blade (gap setting 100 µm), these solutions were casted onto microscope slides (Assistant, Lot.: 3204284, ≈76 × 26 mm^2) that were subsequently placed in 2 L deionized water. The opaque films were subsequently air dried, placed in clip holder device, and UV–vis spectra were recorded using an integrating sphere.

Transparent CAPh/dye films were prepared by regeneration from DMA by solvent evaporation. For films with a dye content > 1.5 wt%, the required amount of SB was directly added to 1 mL of a CAPh stock solution (0.4 mol L^{-1}) in acetone. For films with a dye content < 1.5 wt%, defined volumes of an SB stock solution (0.011 mol L^{-1}) in acetone were added into 1 mL CAPh stock solution (0.4 mol L^{-1}) to yield the desired end concentrations. Using a doctor blade (gap setting 100 µm), these solutions were casted onto microscope slides and air dried to remove acetone, which resulted in regeneration of transparent CAPh/dye composite films. The corresponding UV–vis spectra were recorded in transmission mode.

2.4.3. Particle Suspensions and Dye in Bulk

NP suspension **CAPh-4_SB-2**, obtained by dialysis, was diluted with HPLC grade water in the ratios 1:100, 1:200, 1:300, 1:400, and 1:500 (v/v) and measured in the center of an integrating sphere on a PerkinElmer Lambda 950 UV–vis using quartz class cuvettes polished on four sides. For recording the UV–vis spectra of SB in bulk, given amounts of the dye (1.14, 0.57, and 0.11) were dissolved in 2.5 mL acetone. The solutions were filled into four side polished quartz glass cuvettes and the solvent was evaporated first in a nitrogen stream and subsequently in vacuum at 70 °C. The dye coated cuvettes were placed and measured in the center of an integrating sphere.

2.5. Immunoassay

For all of the following experiments, reverse osmosis grade water was employed.

2.5.1. Nanoparticle Protein Conjugate Preparation

A volume of 1 mL of the aqueous CAPh/dye NP dispersions was adjusted to pH 5.5 by addition of 100 µL MES buffered solution. EDC/sulfo-NHS activation of the carboxyl groups was carried out by adding 10 mg of each reagent to the dispersion and shaking the mixture for 30 min. Centrifugation and resuspension in PB buffered solution (0.03 mol L^{-1}, pH 7.3) was performed at 10 000 g for 15 min to remove the excess of EDC and sulfo-NHS. Covalent antibody immobilization was performed by incubation of 300 µg anti-h CRP 6405 antibody with the activated NP in 1 mL PB buffered solution (0.03 mol L^{-1}, pH 7.3) for 2 h at 25 °C. By the addition of 10 µL ethanolamine and shaking for 60 min, excess binding sites were blocked. After antibody immobilization, not bound antibodies were removed by centrifugation. The final volume of the NP suspension was adjusted to 100 µL by adding PBS buffered solution containing BSA (10 mg mL^{-1}).

2.5.2. Preparation of Lateral Flow Assay Test Strips

A detailed description of the fabrication and optimization of lateral flow assay strips is provided in the Supporting Information. In brief, the test strips were comprised of a sample pad, a conjugate pad, nitrocellulose membrane, and an absorbent pad. After the membrane and the absorbent pad were attached onto the backing card, capture antibody solution (anti-CRP 6404, 250–1250 µg mL^{-1}) and goat anti-mouse IgG antibody solution (1000 µg mL^{-1}) in PB buffer (0.3 mol L^{-1}, pH 7.3) were dispensed in different zones (test line and control line) on the nitrocellulose membrane by a dispenser system (BioJet Quanti 3000, 1 µL antibody solution cm^{-1}). Subsequently, the dispensed membrane was dried at 37 °C for 2 h. The NP antibody conjugates were diluted to different antibody concentrations (80–400 µg antibody mL^{-1}) in a PB buffer (0.03 mol L^{-1}, pH 7.3, 1% BSA, 1% sucrose) and these suspensions were dispensed (10 µL cm^{-1}) in a glass fiber membrane with a BioDot XYZ-3000 dispensing platform to obtain antibody loaded conjugate pads. The conjugate pads were dried for 2 h at 37 °C. The loaded conjugate pad and the absorbent pad (untreated glass fiber membrane) were then also attached onto the backing card and cut into test stripes (4 × 60 mm).

2.5.3. Procedure of Lateral Flow Assay

CRP solutions of various concentrations were prepared in a PBS running buffer (pH 7.3 containing 25% CBC, 0.05% Tween 20). A volume of 100 µL of the CRP solutions was added to the sample pad of a test strip. After 10 min, the color intensity at the test line of the strips was measured using ESE Quant lateral flow reader (Qiagen). Using origin 8.0 software, the intensity of the optical signal was fitted with the basic 4-parameter-logistic (4PL).[17] Limit of detection (LOD) was estimated as the concentration of CRP corresponding to a signal intensity of 30 mV of this measurement. The linear working range was determined as the concentrations starting from the LOD up to the concentration causing 90% of the maximal assay signal. The 50% inhibition (IC_{50}) value related to the midpoint of the curve was calculated.

3. Results and Discussion

3.1. Polysaccharide Based Nanoparticles

In a first set of experiments, the formation of cellulose ester NP in the absence of dye molecules was studied. CAPh was used in this study, which is a hydrophobic mixed ester with carboxyl groups. The carboxyl groups enable covalent and/or electrostatic linkage with antibodies, which was a basic requirement for the targeted immunoassay applications. In addition, CA as a noncharged cellulose ester was included in the study in order to evaluate the effect of the charged carboxyl moiety on particle properties and dye incorporation. Both derivatives were dissolved in DMA at concentrations of 1–8 mg mL^{-1} and dialyzed against the nonsolvent water to yield turbid particle dispersions that were characterized with respect to morphology, particle size, PDI, and ζ-potential (Table 1). Independent of the cellulose ester concentration, CAPh, which is an anionic polysaccharide derivative, formed nm-scaled particles with a regular spherical shape very similar to previously reported particles obtained by dialysis of noncharged and cationic polysaccharide derivatives (Figure 1).[7,10] The SEM images also displayed a small content of elongated particles. It is unlikely that these were formed during the dialysis since the majority of particles, which determines the macroscopic particle properties, showed a regular shape. The sample preparation for SEM imaging includes a drying step that might have induced a fusion of multiple particles that were in close vicinity. Similar "misshapes" can be seen in SEM images of NP derived from other polysaccharide derivatives.[3,6,10]

With increasing polymer concentration, CA NP increased in size from 281 nm (2 mg mL^{-1}) to a threshold of 370–390 nm (≥ 4 mg mL^{-1}). In case of CAPh, an increase in concentration resulted in a gradual increase of the particle size from 293 nm (2 mg mL^{-1}) to 484 nm (8 mg mL^{-1}) without reaching a plateau in the concentration range studied. Apparently, the formation of large particles is favored if a higher concentration of cellulose esters is present during the self-assembling process. This corresponds well with previous work of mixed cellulose esters, which have been shaped into NP.[7,18] It is also in accordance with mechanisms of NP formation by nucleation and growth as well as nucleation and aggregation.[19] Supersaturation of the polymer solution proceeds during dialysis and macromolecules nucleate due to concentration fluctuations (nucleation). The initial nuclei grow either by adsorbing further macromolecules from solution (growth) or by aggregation with other nuclei caused by a sufficient number of nuclei in the medium. Thus, mean particle diameter and size distribution increases with increasing polymer concentration.

The concentration of CA had a less pronounced effect on the polydispersity (PDI ≈ 0.13) and mean ζ-potential (≈–30 mV). In case of CAPh, a gradual increase in ζ-potential from ≈–34 mV (2 mg mL^{-1}) to ≈–46 mV (8 mg mL^{-1}) was observed upon increasing concentration. CAPh bears negatively charged moieties and the fact that the particles become increasingly negatively charged might correlated with their surface area that also increases by a factor of roughly three (not taking into account the thickness of the electrolytic double layer).

Table 1. Conditions for and results of the formation of particle suspensions in water from cellulose esters.

ID	Cellulose ester[a)]		Particle properties		
	Type	Concentration [mg mL^{-1}]	Z-average [nm]	PDI	ζ-potential [mV]
CA-2	CA	2	281 ± 3	0.14	–29
CA-4	CA	4	387 ± 2	0.13	–28
CA-6	CA	6	393 ± 4	0.11	–29
CA-8	CA	8	372 ± 4	0.14	–32
CAPh-2	CAPh	2	293 ± 6	0.08	–34
CAPh-4	CAPh	4	336 ± 2	0.13	–40
CAPh-6	CAPh	6	434 ± 4	0.18	–43
CAPh-8	CAPh	8	484 ± 7	0.14	–46

[a)]CA: cellulose acetate, CAPh: cellulose acetate phthalate dissolved in *N,N*-dimethylacetamide.

3.2. Polysaccharide Ester-Dye Composite Nanoparticles

A basic requirement for the preparation of dye loaded composites NP using the dialysis approach is the solubility of the dyes in dipolar aprotic solvents and

Macromol. Chem. Phys. **2016**, DOI: 10.1002/macp.201600160

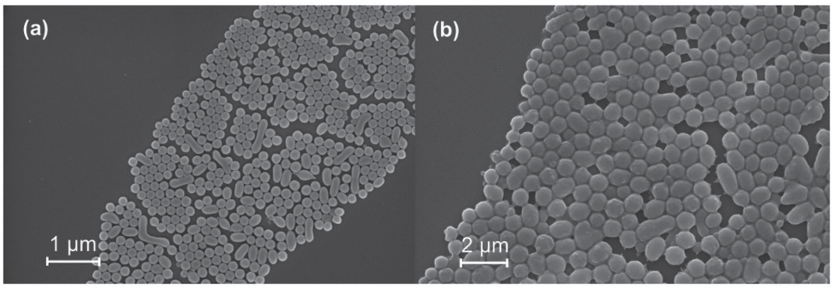

Figure 1. Scanning electron microscopy images of nanoparticles obtained by dialysis of cellulose acetate phthalate (CAPh) dissolved in *N*,*N*-dimethylacetamide against water: a) **CAPh-2**, 2 $mg_{polymer}$ mL^{-1}; b) **CAPh-4**, 4 $mg_{polymer}$ mL^{-1}.

insolubility in water. Three suitable dyes, namely AA, SIV, and SB, were selected for the incorporation into CA and CAPh (Figure 2). They are representatives of two major classes of dyes, anthraquinones (AA) and azo dyes (SIV and SB), and feature deep dark colors that can easily be detected visually due to the strong contrast with the white lateral flow immunoassay test stripes. Mixed solutions of a cellulose derivative and the respective dye in DMA at certain ratios were prepared and subsequently dialyzed against the nonsolvent water (Table 2). AA containing solutions remained transparent for about 15 min before slowly forming a turbid particle suspension, which is comparable to the self-assembling of the cellulose ester NPs that became visible after 10 min (CA) and 15 min (CAPh). In the case of SIV, however, formation of a turbid dispersion was observed already after about 5 min indicating a much faster self-assembling. For SB, a visual distinction was not possible due to the deep color of the system at the amounts employed.

In all cases, deeply colored particle dispersions were obtained that were stable against sedimentation and physical stress (e.g., agitation, centrifugation). No discoloration of the particles occurred that might have indicated a chemical conversion or leaking of dyes into the water phase. Although these findings were expected for the dyes chosen, incorporation of other compounds that are more hydrophilic and/or susceptible for hydrolysis might give different results. High amounts of dyes, up to a ratio of 1 $g_{dye}/g_{cellulose\ ester}$, could be loaded into the composite particles. Dialysis of the dissolved dye without the hydrophobic cellulose esters resulted in an agglomeration and precipitation, which indicated that the dyes are incorporated into a stabilizing matrix of the cellulose esters. The dye loaded composite particles had a spherical shape, similar to the morphology of cellulose ester particles (Figure 3a,b). Cryo-TEM imaging indicated no clear phase separation within the particles (Figure 3c,d).

Incorporation of AA into CA particles led to similar particle sizes and ζ-potentials for the composite particles in comparison to CA NPs. At low cellulose ester concentrations of 2 mg mL^{-1} (**CA-2_AA-1** and **CA-2_AA-2**), the composite particles exhibited a mean diameter around 270 nm and a ζ-potential around –29 mV, which is comparable to pure **CA-2** NP. However, the PDI increased from ≈0.14 (without AA) to ≈0.20, i.e., the size distribution became broader. A similar effect could be observed at higher cellulose ester concentrations (**CA-4_AA-2**), which yielded particles with a mean diameter of 331 nm and ζ-potentials of –33 mV similar to **CA-4** particles. The size distribution broadened only slightly, as indicated by an increase in PDI from 0.13 (**CA-4**) to 0.21 (**CA-4_AA-2**). Apparently, AA has little effect on the self-assembling process of CA based composite particles. Incorporation of AA into CAPh particles slightly affects the particle properties. Composite particles prepared at low cellulose concentrations of 2 mg mL^{-1} (**CAPh-2_AA-1** and **CAPh-2_AA-2**) displayed slightly smaller mean diameters around 200 nm compared to **CAPh-2** particles while the PDI remained comparable around 0.07–0.08 indicated a similar size distribution. The ζ-potential was nearly constant at about –34 mV. At higher cellulose concentrations of 4 mg mL^{-1}, no increase of the particle size was observed upon AA incorporation, which is in contrast to the results obtained with the two sudan dyes. However, the composite particles showed a broader size distribution. The absolute value of ζ-potential of –40 mV (**CAPh-4**) decreased to a threshold of about –33 mV. The primary amine moieties of incorporated AA might interact with carboxyl groups of CAPh possibly leading partly to

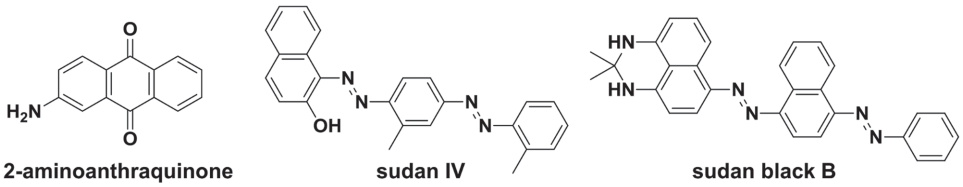

Figure 2. Structure and spectral properties, recorded in *N*,*N*-dimethylacetamide, of dyes used for incorporation into cellulose ester nanoparticles.

Table 2. Conditions for and results of the formation of composite particle suspensions in water from cellulose esters with different dyes.

ID	Cellulose ester[a)]		Dye[b)]			Particle properties		
	Type	Concentration [mg mL^{-1}]	Type	Concentration [mg mL^{-1}]	wt% [%]	Z-average[c)] [nm]	PDI	ζ-potential [mV]
CA-2_AA-1	CA	2	AA	1	33	270 ± 2	0.18	−29
CA-2_AA-2	CA	2	AA	2	50	269 ± 2	0.21	−29
CA-4_AA-2	CA	4	AA	2	33	394 ± 3	0.24	−30
CA-2_SIV-0.5	CA	2	SIV	0.5	20	329 ± 6	0.18	−28
CA-2_SIV-1	CA	2	SIV	1	33	445 ± 2	0.15	−31
CA-2_SIV-2	CA	2	SIV	2	50	620 ± 2	0.14	−30
CA-4_SIV-1	CA	4	SIV	1	20	624 ± 4	0.37	−31
CA-4_SIV-2	CA	4	SIV	2	33	639 ± 6	0.19	−31
CA-4_SIV-4	CA	4	SIV	4	50	762 ± 24	0.17	−30
CA-2_SB-0.5	CA	2	SB	0.5	20	583 ± 11	0.22	−27
CA-2_SB-1	CA	2	SB	1	33	1285 ± 32	0.28	−27
CA-2_SB-2	CA	2	SB	2	50	1455 ± 61	0.26	−27
CA-4_SB-1	CA	4	SB	1	20	1011 ± 14	0.21	−30
CA-4_SB-2	CA	4	SB	2	33	1554 ± 46	0.36	−30
CA-4_SB-4	CA	4	SB	4	50	1911 ± 36	0.30	−26
CAPh-2_AA-1	CAPh	2	AA	1	33	206 ± 2	0.07	−34
CAPh-2_AA-2	CAPh	2	AA	2	50	204 ± 1	0.08	−36
CAPh-4_AA-2	CAPh	4	AA	2	33	331 ± 1	0.21	−33
CAPh-2_SIV-1	CAPh	2	SIV	1	33	798 ± 55	0.25	−27
CAPh-2_SIV-2	CAPh	2	SIV	2	50	910 ± 41	0.25	−28
CAPh-4_SIV-1	CAPh	4	SIV	1	20	677 ± 16	0.24	−37
CAPh-4_SIV-2	CAPh	4	SIV	2	33	768 ± 25	0.21	−34
CAPh-4_SIV-4	CAPh	4	SIV	4	50	735 ± 17	0.28	−31
CAPh-2_SB-0.5	CAPh	2	SB	0.5	20	233 ± 4	0.09	−33
CAPh-2_SB-1	CAPh	2	SB	1	33	321 ± 5	0.26	−33
CAPh-2_SB-2	CAPh	2	SB	2	50	308 ± 3	0.24	−33
CAPh-4_SB-1	CAPh	4	SB	1	20	437 ± 6	0.26	−39
CAPh-4_SB-2	CAPh	4	SB	2	33	355 ± 2	0.20	−38
CAPh-4_SB-4	CAPh	4	SB	4	50	445 ± 5	0.26	−39

[a)]CA: cellulose acetate, CAPh: cellulose acetate phthalate dissolved in ***N*,*N***-dimethylacetamide; [b)]AA: 2-aminoanthraquinone, SIV: sudan IV, SB: sudan black B dissolved in ***N*,*N***-dimethylacetamide; [c)]Mean values of three measurements ± standard deviation.

a masking effect of carboxyl groups by adjunct AA molecules and to a reduction of the ζ-potential.[20]

In comparison to AA, incorporation of SIV into CA and CAPh particles led to significantly altered particle sizes. The mean diameter of CA-SIV composite particles prepared at low cellulose ester concentration of 2 mg mL^{-1} (**CA-2_SIV-0.5**, **CA-2_SIV-1**, and **CA-2_SIV-2**) increased continuously from 329 to 620 nm with increasing dye concentration (0.5 to 2 mg mL^{-1}), which is significantly higher compared to **CA-2** NP (281 nm). At higher cellulose ester concentration of 4 mg mL^{-1}, composite particles (**CA-4_SIV-1**, **CA-4_SIV-2**, and **CA-4_SIV-4**) exhibited even larger diameters of 624–762 nm. For CAPh–SIV composites a comparable trend for the particle sizes was observed. The diameters increased from around 300 nm (**CAPh-2** and **CAPh-4**) to around 700–900 nm upon dye incorporation. Apparently, SIV disturbs the self-assembling of cellulose esters into uniform nanoscaled particles, which

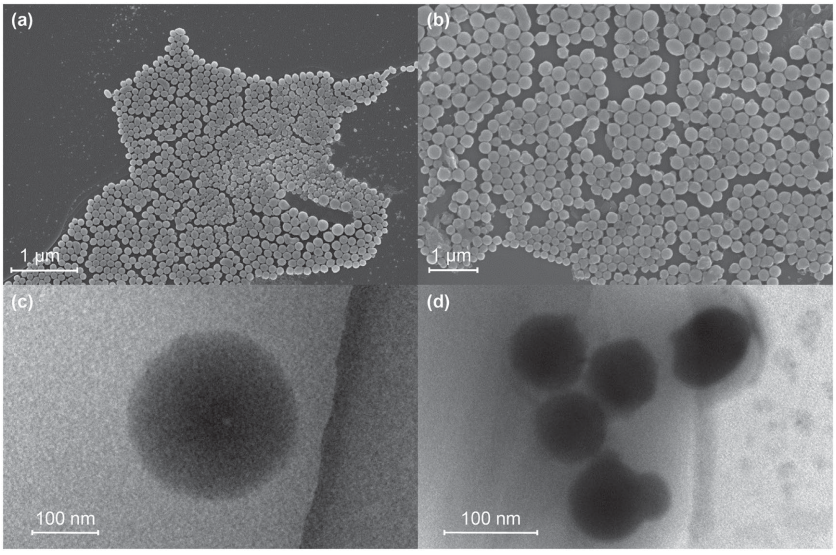

Figure 3. a,b) Scanning electron microscopy and c,d) cryo transmission electron microscopy images of composite nanoparticles obtained by dialysis of cellulose acetate phthalate (CAPh)/sudan black B (SB) solutions in *N*,*N*-dimethylacetamide with concentrations of 2 $mg_{polymer}$ mL^{-1} and 0.5 mg_{dye} mL^{-1} (a/c; **CAPh-2_SB-0.5**) as well as 4 mg_{polyer} mL^{-1} and 2 mg_{dye} mL^{-1} (b/d; **CAPh-4_SB-2**).

is also indicated by the broader size distribution of SIV-composite particles; the PDI increased from around 0.13 for the cellulose ester NP (CA and CAPh) to 0.21–0.28 for CAPh_SIV NP and 0.14–0.37 for CA_SIV NP. The ζ-potential of CA NP remained nearly unchanged upon SIV incorporation at about –30 mV. In case of CAPh NPs, a decrease in the absolute value of the ζ-potential was observed for CAPh_SIV composite NP. This might be an effect of the less favorable self-assembling of CAPh, i.e., a decrease in the density of carboxylic groups near the NP surface, as opposed to the masking effect of AA.

Overall, CA and CAPh derived particles displayed similar trends upon incorporation of AA and SIV with the exception that the ζ-potential remained almost constant below –30 mV for CA composite particles and slightly increased by about +5 mV for CAPh composite particles depending on the amount of dye added. Thus, it can be concluded that the negatively charged carboxyl group has little effect on the incorporation of AA and SIV within the composite particles. The main difference seems to derive from the hydrophobicity of these dyes that can be expressed quantitatively by their *n*-octanol/water partition coefficients (log *P*).[21] NP formation through solvent displacement can be ascribed to two mechanisms, (i) nucleation and growth and (ii) nucleation and aggregation.[7,19] In both processes, the affinity of the two different components (cellulose ester and dye) towards the hydrophobic nuclei is an important factor. SIV is a highly hydrophobic compound (log P_{SIV} = 8.72) and it can be expected that even the presence of small amounts of water will induce aggregation of the dye in solution. Particle formation would proceed from these aggregates leading to bigger and less uniform particles. This hypothesis is supported by the finding that the formation of SIV composite particles is much faster (≈5 min), i.e., it occurs under less controlled conditions, compared to the formation of CA and CAPh as well as AA composite particles (≈15 min). However, it could not be deduced whether SIV starts to agglomerate prior to the self-assembling of the cellulose esters or at the same time. AA (log P_{AA} = 3.31) is less hydrophobic and more similar to the two cellulose esters employed in terms of solubility and aggregation behavior. As a results, the presences of AA apparently has only a little effect on the self-assembling process of CA and CAPh into NP, which results in comparable particle properties of cellulose ester NP and AA composite NP.

Significant differences between the two cellulose esters were observed in case of SB composites. Loading of CA particles with SB induced a dramatic increase in particle diameters to > 1 µm and broad size distributions > 0.20 at both cellulose ester concentrations (2 and 4 mg mL^{-1}) except for **CA-2_SB-0.5** (2 $mg_{polymer}$ mL^{-1} and 0.5 mg_{dye} mL^{-1}) with 583 nm. A similar but less pronounced trend was already observed for SIV composite particles, which can be attributed to the strong hydrophobicity of both dyes (log P_{SIV} = 8.72, log P_{SB} = 8.81).[21] The mean ζ-potentials of CA-SB particles were comparable to those of CA NP prepared at the same polymer concentration (≈–27 mV at 2 mg mL^{-1}, ≈–30 mV at 4 mg mL^{-1}. Surprisingly, incorporation of SB into CAPh particles did not result in a significant increase in particle size. At low cellulose ester concentration (2 mg mL^{-1}), dye loaded CAPh composite particles with diameters around 230–320 nm and ζ-potentials of –33 mV were obtained, which is comparable to the corresponding **CAPh-2** particles (293 nm, –34 mV). Also at a cellulose ester concentration of 4 mg mL^{-1}, no significant difference between CAPh and CAPh-SB particles was observed. Independent of the SB concentration, particle sizes around 350–450 nm and ζ-potentials in the range from –38 to –40 mV were observed. Comparably to SIV, SB is highly hydrophobic (log P_{SB} = 8.81), which will strongly affect the self-assembling process of CA and SB during dialysis against water. However, SB also features secondary amino groups that can interact with the carboxyl groups of CAPh by hydrogen bonding and, thus, partly compensate the effect of the strong hydrophobicity of the dye.

3.3. UV–Vis Characterization

The UV–vis spectroscopic properties of dye loaded composite NP are important parameters for lateral flow immunoassays that rely on optical detection of antibody label particles. Moreover, UV–vis spectroscopy can provide valuable information on the incorporation of hydrophobic dyes within the cellulose ester matrix. Depending on how the dye interacts with the surroundings, the spectroscopic properties of the composite particles will be determined by interaction of the chromophore with itself (dye–dye), the cellulose ester (dye–matrix), and the surrounding aqueous medium (dye–water). These individual effects were assessed separately by different experiments. SB has the highest extinction coefficient among the dyes tested and the corresponding CAPh composite particles were found to be the most promising candidates for immunoassay applications. Thus, CAPh-SB particles were chosen for detailed UV–vis spectroscopic characterization.

In a first set of experiments, UV–vis spectra of SB dissolved in DMA/water mixtures with different ratios ranging from 10:0 to 1:9 (v/v) were recorded at constant concentration (2.0×10^{-5} mol L^{-1}, Figure 4a). The overall absorption decreased with increasing water content while the wavelength of the maxima exhibited a hypsochromic shift. Extrapolation to 100% water yielded $\lambda_{max} = 580$ nm compared to 628 nm in pure DMA (see Figure 4b). This decrease is related to the fact that the solvent's ability to form hydrogen bonds increases upon successive replacement of DMA (poor hydrogen bond donor) by water (strong hydrogen bond donor). More pronounced stabilization of the ground state by hydrogen bond interaction with the solvent will result in a shift of the adsorption maximum to lower wavelengths. This postulation is in accordance with the literature in which a similar hypsochromic shift has also been observed using alcohols with increasing hydrogen bond acidity as solvents for SB instead of dipolar aprotic solvents.[22] Estimated absorption maximum of SB in water (580 nm) is slightly lower than the one reported for methanol (589 nm), which is reasonable since water is an even stronger hydrogen bond donor, i.e., the hypsochromic shift becomes more pronounced.

In solution, the optical properties of SB are strongly affected by interaction with the solvent, in particular water. UV–vis measurement of solid SB in the integrating sphere allows determination of spectroscopic properties without any interaction of surrounding media as illustrated in Figure 4c. The absorption maximum is located at 600 nm, which is situated between the absorption maxima in water (580 nm) and DMA (627 nm).

In order to mimic the interaction of SB with the CAPh matrix, composite films were prepared by dissolving both components in acetone, casting the solutions, and evaporating the solvent. The transparent films were characterized by UV–vis experiments in transmission mode (Figure 5a). The spectral resolution of the absorption curves is lower compared to the measurement in solution, due to fixation of dye molecules inside the rigid CAPh matrix, and therefore the maximum, which is located at 615 nm, became broader. The overall absorbance decreased with decreasing dye content. The second local maximum around 430 nm occurred only as a shoulder at higher concentrations. Films were also obtained by casting CAPh-SB solutions in DMA and subsequent coagulation in an excess of water. This approach is similar to the three-dimensional self-assembling of CAPh and SB into composite NP because it simulates the change from dissolved to solid state by the exchange of DMA (solvent) with water (nonsolvent). The films obtained were opaque, which can be attributed to light scattering by polymer coils formed during the slow self-assembling of CAPh. Thus, the spectra were not recorded in transmittance but absorption mode using an integrating sphere as it has been done with colored particle suspensions, which explains the lower resolution (Figure 5b). Nevertheless, an adsorption maximum around 620 nm could be determined, which corresponds to the value obtained for the

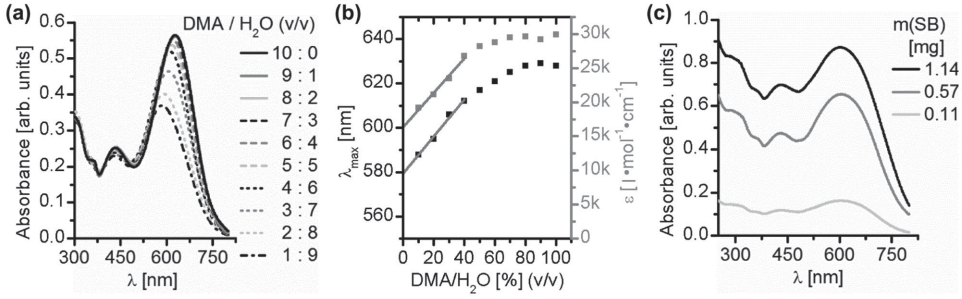

Figure 4. a) UV–vis spectra of sudan black B (SB) with a same concentration of 2.0×10^{-5} mol L^{-1} dissolved in *N*,*N*-dimethylacetamide (DMA)/water mixtures with different ratios from 10:0 to 1:9 (v/v). b) Correlation of absorption maximum wavelengths (left *y*-axis) and extinction coefficients (right *y*-axis) with water content of DMA/water mixtures. c) UV–vis spectra of solid SB measured with different total masses in the measuring cell.

Macromol. Chem. Phys. **2016**, DOI: 10.1002/macp.201600160

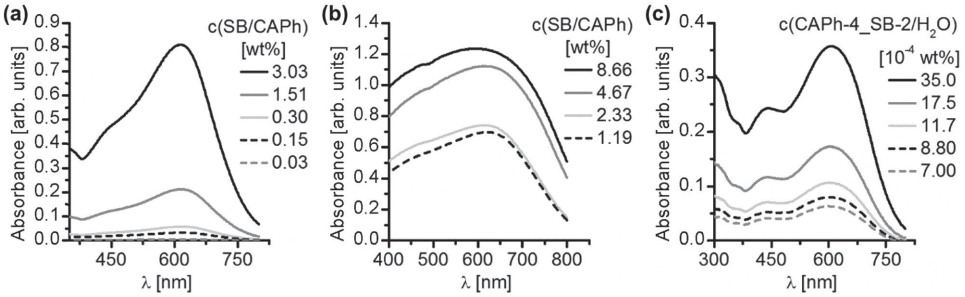

Figure 5. UV–vis spectra of sudan black B (SB) embedded in cellulose acetate phthalate (CAPh) films with different SB/CAPh mixing ratios a) casted from acetone and air-dried as well as b) casted from *N*,*N*-dimethylacetamide and coagulated in water. c) UV–vis spectra of CAPh-SB composite nanoparticle suspensions with different mass concentrations.

transparent films. Compared to the solid dye, the adsorption maximum of SB within the CAPh composite films exhibited a bathochromic shift of about 20 nm. This can be attributed to a pronounced interaction of the dye with the surrounding CAPh matrix. It can be speculated that this interaction is similar to the polar interaction of dissolved SB in DMA (627 nm), which stabilizes the excited state of the dye and bathochromically shifts the absorption. The bathochromic shift was less pronounced for the film with the highest SB content (8.66 wt%). Thus, it can be concluded that the effect of dye–matrix interactions decreases with an increasing amount of dye within the composites.

NP suspension **CAPh-4_SB-2** was investigated using UV–vis spectroscopy. For this purpose, the stock suspension was diluted to different mass concentrations and measured using an integrating sphere (Figure 5c). The spectra recorded strongly resembled those of the solid dye. In both cases, the adsorption maxima were located around 600 nm. Thus, it can be concluded that the spectroscopic properties of the CAPh-SB-composite particles are primarily determined by dye–dye interactions while interaction with the surrounding matrix as well as water on the particle surface seem to be negligible. It can be speculated that instead of forming a continuous homogeneous matrix, SB is enriched in the interior of the particle while CAPh is concentrated the outer layer. This would also correspond with the fact that CAPh and CAPh-SB composite particles exhibited similar ζ-potentials. However, TEM images revealed no clear phase separation within the particles, i.e., the particles most likely feature a gradual distribution of both components along the lateral cross section instead of a defined core-shell-structure (Figure 3c,d).

3.4. Immunoassay Tests

The dye loaded CAPh composite particles feature reactive carboxyl groups that can be employed for covalent or adsorptive coupling of additional functionalities such as antibodies. In the present work, the carboxyl groups were converted into the activated sulfo-NHS esters and subsequently reacted with CRP specific antibodies via their amino groups. The antibody-particle conjugates obtained were evaluated for their potential use as optical labels in immunoassays.[14] For this purpose, lateral flow assays were constructed and optimized as described in the Supporting Information.

The lateral flow assay tests with different antibody labeled CAPh-dye composite particles were performed by varying the CRP concentration in the sample from 0 to 64 ng mL^{-1} (Figure 6). The different NP conjugates were compared with respect to the LOD of the assay that was defined here as the minimum CRP amount where a significant difference in color density of the capture zone in comparison the blank value could be observed visually.

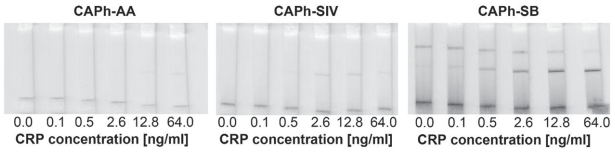

Figure 6. Lateral flow assay test strips for detection of C-reactive protein (CRP) using cellulose acetate phthalate (CAPh) dye composite particles (AA: 2-aminoanthraquinone, SIV: sudan IV, SB: sudan black) coupled with anti-h CRP 6404 as labels.

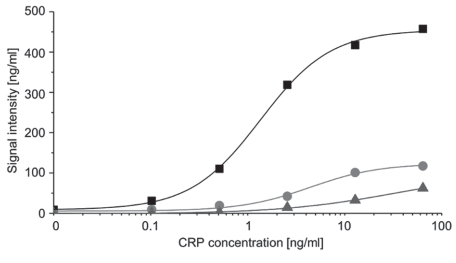

Figure 7. Quantitative optical read out and calibration curves of the lateral flow assay detection of C-reactive protein (CRP) using cellulose acetate phthalate dye composite particles (▲: 2-aminoanthraquinone, ●: sudan IV, ■: sudan black) coupled with anti-h CRP 6404 as labels.

Table 3. Characteristics of the lateral flow assays for detection of C-reactive protein obtained by optical read out.

Composite particles used[a)]	Limit of detection [ng mL^{-1}]	Dynamic working range [ng mL^{-1}]	IC_{50}[b)] [ng mL^{-1}]
CAPh-4_AA-2	9.7	9.7 – 638.4	33.5
CAPh-4_SIV-2	2.2	2.2 – 76.3	60.8
CAPh-4_SB-2	0.15	0.15 – 9.9	1.4

[a)]CAPh: cellulose acetate phthalate, AA: 2-aminoanthraquinone, SIV: sudan IV, SB: sudan black; [b)]IC 50: 50 % inhibition.

With CAPh-AA composite particles (**CAPh-4_AA-2**), a visible LOD of 12.8 ng CRP mL^{-1} was achieved. A slightly more sensitive test, i.e., lower visual LOD of 2.6 mg, was achieved by using CAPh-SIV composite particles (**CAPh-4_SIV-2**), which is probably due to the higher extinction coefficient of SIV. The best results were obtained with CAPh-SB conjugates (**CAPh-4_SB-2**) that could detect CRP down to a visual LOD of 0.1 ng mL^{-1}, which is very sensitive compared to conventional detection methods. Typical LOD for proteins in lateral flow assay are around 1 ng protein mL^{-1}.[23] As an example, a CRP assay with a LOD of 0.69 ng CRP mL^{-1} has been reported that employed colloidal gold particles that are most commonly employed as labels in immunoassay applications.[24] Thus, the newly developed CAPh-SB particles are well suited for developing competitive immunoassay applications.

To obtain quantitative results and verify the visual LOD, color intensities of the test lines were evaluated using a lateral flow reader. The mean signal values were fitted to a sigmoid equation and displayed as the standard curve (Figure 7). From these data, characteristic parameters that describe the assays efficiency were determined (Table 3). CAPh-SB particle yielded a very low LOD of 0.15 ng CRP mL^{-1}, which correlates well with the semi-quantitative visual read out. Apparently, the strong contrast between black (dye particles) and white (test strip) allows a very sensitive visual detection, which is required in rapid test systems. The measurable dynamic range in which CRP can be detected quantitatively with an assay that is based on these particles ranges from 0.15 to 9.9 ng CRP mL^{-1}. As has been observed visually, quantitative analysis demonstrated that CAPh-SIV and CAPh-AA composite particles were less sensitive labels for CRP detection. Depending on the specifics of the antigen that needs to be detected, CAPh-dye composite particles can be used as labels in lateral flow immunoassays tests both on a semi-quantitative (visual read out) as well as quantitative level (optical read out). As an example, the clinically relevant CRP in human serum ranges from 0–1 μg mL^{-1} in healthy persons without any signs of inflammation to > 10 μg mL^{-1} for persons with minor infections.[25] This range can easily be targeted with the dye composite prepared, e.g., by dilution of the biological samples.

4. Conclusions

Hydrophobic dye molecules could be incorporated into NPs prepared by self-assembling of hydrophobic cellulose esters. It was demonstrated that particle properties of the composites are affected by the hydrophobicity of the dyes as well as secondary interactions such as hydrogen bonding between the dye and the polysaccharide ester matrix. UV–vis spectroscopic measurements suggested that in particular highly hydrophobic dyes are not evenly but gradually distributed within the composite particles. This finding will be of great importance also for the incorporation of other types of active compounds such as drug molecules into polysaccharide based nanomaterials.

Exploiting their reactive carboxyl group, it was possible to couple CAPh based composite particles with CRP antibodies. The colored conjugates obtained were well suited for the application as labels in lateral flow immunoassays. Based on the knowledge gained, future studies will be expanded in different ways. Other test systems of clinical relevance will be established by including other types of antibodies. It is also possible to tailor the sensitivity and dynamic working range of the lateral flow assay by incorporating other dyes (e.g., florescent ones) and/or multiple dyes using the approach established in this work. Moreover, by tailoring the molecular structure of the self-assembling polysaccharide derivative that forms the matrix of the composite NP, it is possible to tailor the physical properties and the surface chemistry of the composite particles.

Supporting Information

Supporting Information is available from the Wiley Online Library or from the author.

Acknowledgements: P.S., M.G., H.W., and T.H. are members of the European Polysaccharide Network of Excellence (EPNOE), www.epnoe.eu. This work was partely funded by the German Federal Ministry of Food and Agriculture based on an enactment of the German Bundestag. It is part of the activities of the PShapes project (www.bioshapes.net/) conducted under the framework of the joint trans-national WoodWisdom-Net Research Program

(www.woodwisdom.net). P.S. and P.M. acknowledge the financial supported from the German Federal Ministry for Economic Affairs and Energy (INNO-KOM-OST MF 140179). The authors thank M. v. d. Lühe and S. Stumpf, both Institute of Organic Chemistry and Macromolecular Chemistry/Jena Center for Soft Matter (FSU Jena) for TEM and SEM measurements.

Received: April 11, 2016; Revised: May 23, 2016; Published online: ; DOI: 10.1002/macp.201600160

Keywords: cellulose esters; hydrophobic dyes; immunoassay; nanoparticles; polysaccharides

[1] T. Heinze, S. Hornig, in *Polysaccharide Materials: Performance by Design* (Eds.: K. J. Edgar, T. Heinze, C. M. Buchanan), American Chemical Society, Washington, DC **2009**, p. 169.
[2] H. Wondraczek, T. Elschner, T. Heinze, *Carbohydr. Polym.* **2011**, *83*, 1112.
[3] E. Aschenbrenner, K. Bley, K. Koynov, M. Makowski, M. Kappl, K. Landfester, C. K. Weiss, *Langmuir* **2013**, *29*, 8845.
[4] A. Geissler, D. Scheid, W. Li, M. Gallei, K. Zhang, *Cellulose* **2014**, *21*, 4181.
[5] S. Hornig, T. Heinze, *Carbohydr. Polym.* **2007**, *68*, 280.
[6] M. R. Kulterer, M. Reischl, V. E. Reichel, S. Hribernik, M. Wu, S. Köstler, R. Kargl, V. Ribitsch, *Colloids Surf., A* **2011**, *375*, 23.
[7] H. Wondraczek, K. Petzold-Welcke, P. Fardim, T. Heinze, *Cellulose* **2013**, *20*, 751.
[8] E. M. Bachelder, T. T. Beaudette, K. E. Broaders, J. Dashe, J. M. J. Fréchet, *J. Am. Chem. Soc.* **2008**, *130*, 10494.
[9] S. Hornig, C. Biskup, A. Grafe, J. Wotschadlo, T. Liebert, G. J. Mohr, T. Heinze, *Soft Matter* **2008**, *4*, 1169.
[10] M. Nikolajski, J. Wotschadlo, J. H. Clement, T. Heinze, *Macromol. Biosci.* **2012**, *12*, 920.
[11] S. Daus, T. Heinze, *Macromol. Biosci.* **2010**, *10*, 211.
[12] M. Obst, T. Heinze, *Macromol. Mater. Eng.* **2016**, *301*, 65.
[13] Y. Wang, T. Heinze, K. Zhang, *Nanoscale* **2016**, *8*, 648.
[14] X. Pei, B. Zhang, J. Tang, B. Liu, W. Lai, D. Tang, *Anal. Chim. Acta* **2013**, *758*, 1.
[15] K. J. Edgar, *Cellulose* **2006**, *14*, 49.
[16] T. Liebert, T. Heinze, *Biomacromolecules* **2005**, *6*, 333.
[17] J. W. A. Findlay, R. F. Dillard, *AAPS J.* **2007**, *9*, E260.
[18] S. Hornig, T. Heinze, *Biomacromolecules* **2008**, *9*, 1487.
[19] J. Aubry, F. Ganachaud, J.-P. Cohen Addad, B. Cabane, *Langmuir* **2009**, *25*, 1970.
[20] T. Musumeci, C. A. Ventura, I. Giannone, B. Ruozi, L. Montenegro, R. Pignatello, G. Puglisi, *Int. J. Pharm.* **2006**, *325*, 172.
[21] Physical/Chemical Property Database (PHYSPROP), http://esc.syrres.com/fatepointer/search.asp (accessed: February 2016).
[22] M. S. Zakerhamidi, S. G. Sorkhabi, A. N. Shamkhali, *Spectrochim. Acta, Part A* **2014**, *127*, 340.
[23] G. A. Posthuma-Trumpie, J. Korf, A. van Amerongen, *Anal. Bioanal. Chem.* **2009**, *393*, 569.
[24] Y. K. Oh, H.-A. Joung, H. S. Han, H.-J. Suk, M.-G. Kim, *Biosens. Bioelectron.* **2014**, *61*, 285.
[25] S. McWilliam, A. Riordan, *Arch. Dis. Child. Educ. Pract. Ed.* **2010**, *95*, 55.